

See discussions, stats, and author profiles for this publication at: <https://www.researchgate.net/publication/263397632>

# Full-Electron Ligand-to-Ligand Charge Transfer in a Compact Re(I) Complex

ARTICLE in THE JOURNAL OF PHYSICAL CHEMISTRY A · JUNE 2014

Impact Factor: 2.69 · DOI: 10.1021/jp5039877 · Source: PubMed

CITATIONS

3

READS

13

7 AUTHORS, INCLUDING:



Yuankai Yue

Tulane University

7 PUBLICATIONS 25 CITATIONS

SEE PROFILE



Zheng Ma

Duke University

6 PUBLICATIONS 15 CITATIONS

SEE PROFILE



Russell H Schmehl

Tulane University

125 PUBLICATIONS 4,453 CITATIONS

SEE PROFILE

# Full-Electron Ligand-to-Ligand Charge Transfer in a Compact Re(I) Complex

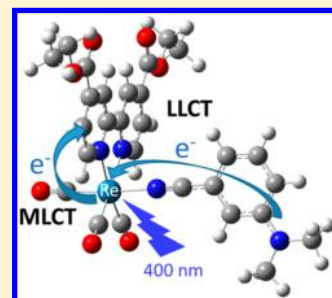
Yuankai Yue,<sup>†</sup> Tod Grusenmeyer,<sup>†</sup> Zheng Ma,<sup>‡</sup> Peng Zhang,<sup>‡</sup> Russell H. Schmehl,<sup>†</sup> David N. Beratan,<sup>‡</sup> and Igor V. Rubtsov<sup>\*,†</sup>

<sup>†</sup>Department of Chemistry, Tulane University, New Orleans, Louisiana 70118, United States

<sup>‡</sup>Departments of Chemistry, Biochemistry, and Physics, Duke University, Durham, North Carolina 27708, United States

## S Supporting Information

**ABSTRACT:** Ligand-to-ligand charge transfer (LLCT) states in transition metal complexes are often characterized by fractional electron transfer due to coupling of the LLCT state with many other states via the metal. We designed and characterized a compact Re<sup>I</sup> complex that displays essentially full-electron charge transfer in the LLCT excited state. The complex, [Re(DCEB)(CO)<sub>3</sub>(L)]<sup>+</sup> (DCEB = 4,4'-dicarboxyethyl-2,2'-bipyridine), referred to as ReEBA, features two redox active ligands with strong electron accepting (DCEB) and electron donating (L is 3-dimethylaminobenzonitrile (3DMABN)) properties. The lowest energy excited state formed with a ca. 10 ps time constant and was characterized as the full-electron 3DMABN → DCEB LLCT state using time-resolved infrared spectroscopy (TRIR), transient absorption spectroscopy, and DFT computations. Analysis of a range of vibrational modes helped to assign the charge transfer characteristics of the complex. The LLCT state lifetime in ReEBA shows a strong dependence on the solvent polarity and features solvent dependent frequency shifts for several vibrational reporters. The formation of a full-electron LLCT state (~92%) was enabled by tuning the redox properties of the electron accepting ligand (DCEB) and simultaneously decoupling the redox active group of the electron donating ligand (3DMABN) from the metal center. This strategy is generally applicable for designing compact transition metal complexes that have full-electron LLCT states.



## 1. INTRODUCTION

The control and manipulation of photoinduced intramolecular charge transfer is of central importance for developing photosensitizers, optical limiters, sensors, and other photonic devices. Donor-bridge-acceptor compounds have been explored for three decades to characterize the structural and dynamical factors that control photoinduced charge separation and recombination (see refs 1–3). Recent interest has focused, as well, on using IR excitation to control charge transfer in small molecules.<sup>4–6</sup>

Transition metal complexes provide a robust scaffold to investigate charge transfer. Complexes of substitutionally inert metals are amenable to modifications and are attractive for performing photoinduced electron–hole separation. Indeed, the characteristic UV–vis absorption spectra of transition metal complexes are often derived from metal-to-ligand and ligand-to-metal charge-transfer transitions (MLCT and LMCT). The distance of the charge shift in MLCT and LMCT states is typically small, and the extent of charge transfer corresponds to less than one electron. Enhancing the oscillator strength for such transitions indeed tends to produce complexes with strongly coupled spatially extended states. Nevertheless, MLCT states can produce charge polarized excited states; further polarization can be achieved by forming ligand-to-ligand charge-transfer states (LLCT) where a complete charge separation can be obtained.<sup>7–9</sup> Here, we show that, by tailoring the properties of two redox active ligands, a LLCT state with essentially full charge separation can be obtained while keeping the compound compact. The electronic decoupling of the metal

center and a ligand is accomplished not by increasing the distance between the redox active centers but by manipulating the electronic coupling interactions and energy matching of the component parts of the complex (metal and ligands).

The specific systems studied are rhenium tricarbonyl diimine complexes, [Re<sup>I</sup>(CO)<sub>3</sub>(N,N)(L)], with luminescent MLCT excited states that have lifetimes of hundreds of nanoseconds.<sup>10–12</sup> Excitation into the singlet MLCT state is followed by relaxation into the triplet MLCT manifold within a few hundred femtoseconds.<sup>13</sup> Note that the fast intersystem crossing occurs due to a strong spin–orbit coupling at the Re metal center; as a result, most states accessed experimentally in this work have a triplet character, which is not indicated explicitly in the notation. A useful handle for observing evolution of the MLCT state is provided by the strong CO stretching modes of these complexes. These CO modes were shown to have a high sensitivity to redistribution of electron density in the excited state, since the CO stretching modes are affected by changes in backbonding from the metal center.<sup>14–18</sup> It is also possible to design derivatives that have functional groups with strong infrared absorption on N,N and/or L that further enhance the ability to track electron density changes during excited-state evolution.<sup>14</sup>

**Special Issue:** Current Topics in Photochemistry

**Received:** April 23, 2014

**Revised:** June 23, 2014

**Published:** June 23, 2014

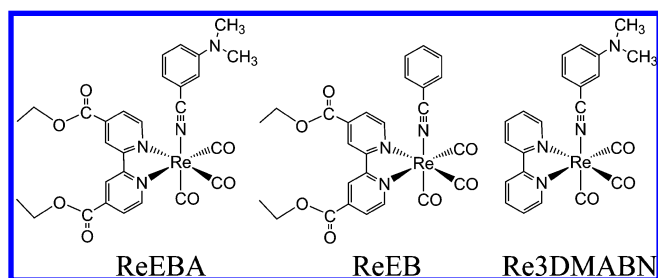


The decay of the initially formed MLCT state and the ability ultimately to form a LLCT state is largely determined by the nature of L. In some instances, L is an easily reduced species that results in redistribution of electron density from the *N,N* ligand to L in the excited state.<sup>19</sup> Examples also exist where L is a strong electron donating ligand, and formation of an L-to-*N,N* ligand-to-ligand charge-transfer (LLCT) state occurs.<sup>8,9,20,21</sup> The rate of the charge migration in these systems can vary from sub-ps to ns time scales and is often strongly solvent dependent.<sup>8,14,22</sup>

These latter systems, in which ligand-to-ligand electron transfer occurs ostensibly to form a fully charge-separated state, have been the subject of numerous studies of photoinduced intramolecular electron transfer (for reviews, see refs 1–3). A key approach to evaluating electron transfer in systems consisting of an electron donor, a chromophore, and an electron acceptor has been to observe quenching of the luminescence of the chromophore concomitant with transient spectral signatures of the oxidized donor and reduced acceptor. We have recently examined  $[\text{Re}^{\text{I}}(\text{CO})_3(\text{N,N})(\text{L})]^+$  compounds with a sufficiently low L oxidation potential to exhibit LLCT ( $\text{L} \rightarrow \text{bpy}$ ) transitions, where L is 3-dimethylaminobenzonitrile (3DMABN) or 4-dimethylaminobenzonitrile (4DMABN).<sup>14,23</sup> The characteristic quenching of the MLCT luminescence is observed, supporting the assignment of intramolecular electron transfer from the DMABN ligand to the *N,N* ligand. However, TRIR studies clearly show that coupling between these ligands and the metal center strongly influences the degree of charge transfer. This coupling is especially strong in  $[\text{Re}(\text{bpy})(\text{CO})_3(4\text{DMABN})]^+$  (Re4DMABN), where a quinoidal resonance structure of the 4DMABN ligand facilitates the interaction. Substantial suppression of the Re–L interaction was achieved by changing the position of the amino group on the phenyl ring from 4 to 3 in  $[\text{Re}(\text{bpy})(\text{CO})_3(3\text{DMABN})]^+$  (Re3DMABN). The reduced coupling, however, results in a higher energy of the coupled state, and an intraligand triplet (<sup>3</sup>IL) localized on 3DMABN is found to be the lowest energy excited state. In order to achieve a LLCT state exhibiting full-electron transfer, its energy needs to be lowered relative to the <sup>3</sup>IL state of the 3DMABN, while maintaining LLCT state decoupling from the MLCT state(s) of the complex.

Here we describe a study of Re(I) tricarbonyl compounds that feature a bpy ligand functionalized with two ester groups (DCEB) (Scheme 1) that serves as an electron accepting

**Scheme 1. Structures of ReEBA, ReEB, and Re3DMABN**



ligand. The electron donating ligand (L) is 3DMABN, which supports state decoupling.<sup>14</sup> In addition to the compound with expected charge separation,  $[\text{Re}(\text{DCEB})(\text{CO})_3(3\text{DMABN})]^+$  (ReEBA), its photoredox inactive analogue,  $[\text{Re}(\text{DCEB})(\text{CO})_3(\text{PhCN})]^+$  (ReEB, PhCN = benzonitrile), was also studied. The measurements were performed in solvents of

different polarities using fs/ps TRIR and nanosecond transient absorption. Vibrational labels placed on different positions of the complex were used to monitor excited-state kinetics. Excited-state assignments were made using a combination of experimental data and the results of DFT computations.

## 2. EXPERIMENTAL DETAILS

### Femtosecond Time-Resolved Infrared Spectroscopy.

The detailed instrumentation and procedures were described previously.<sup>14</sup> In summary, a femtosecond laser beam at 804 nm was split into three parts. One part of the beam was frequency doubled to generate a 402 nm visible excitation beam, which has an energy of ca. 2  $\mu\text{J}$ /pulse. The second part of the beam was used to pump an in-house built optical parametric amplifier (OPA) and a difference frequency generation (DFG) assembly to generate a mid-IR probe beam, which has a spectral width of ca. 200  $\text{cm}^{-1}$  (fwhm). The third part of the fundamental beam, reserved for pumping the second OPA, was not used in this work. A  $\text{CaF}_2$  flow cell with a 150  $\mu\text{m}$  path length was used to circulate the sample solution during the experiment. For TRIR measurement, solutions of 9 mM were prepared with two different solvents: dichloromethane (DCM) and nitromethane (NM). Both spectroscopic grade solvents (Aldrich) were used as received. FTIR spectra were measured for solutions before and after the experiment; only negligible differences were observed.

**Cyclic Voltammetry.** Voltammograms were obtained by using an electrochemical analyzer CH1730A (CH Instruments). The working electrode was a glassy-carbon electrode, the counter electrode was a Pt wire, and the reference electrode was an aqueous Ag/AgCl electrode. Data were collected in acetonitrile and dichloromethane solutions containing 0.1 M TBAPF<sub>6</sub>. Dissolved oxygen was removed from all samples by bubbling with argon gas for 10 min prior to the measurements.

**Nanosecond Spectroscopy.** Nanosecond transient absorption data in the UV and visible spectral regions were recorded with an LKS 60 spectrometer (Applied Photophysics) using a  $\text{Nd}^{3+}$ :YAG laser (Brilliant, Quantel) equipped with second and third harmonic generation units and an optical parametric oscillator (OPOTEK, 420–670 nm) for tunable excitation. Transient absorption spectra were constructed from transient decays collected at 10 nm intervals following pulsed laser excitation. The excitation wavelength used for these complexes was 420 nm. Samples were bubbled with  $\text{N}_2(\text{g})$  for 20 min prior to the measurements.

**Quantum Chemistry Calculations.** The electronic ground state and the lowest energy triplet state of ReEBA and ReEB were computed using density functional theory (DFT) implemented in the Gaussian 09 software package with a B3LYP hybrid functional,<sup>24</sup> 6-31G\*\* basis sets for C, H, O, and N atoms, and the LANL2DZ relativistic effective core potential with an associated basis set for Re. While long-range corrected CAM-B3LYP, LC-wPBE, and wB97X functionals were tested previously for Re3DMABN, Re4DMABN, and ReBN complexes, a better agreement with the experimental vibrational frequencies and electronic spectra was found with the B3LYP functional.<sup>14</sup> The integral equation formalism of the polarizable continuum model as implemented in Gaussian 09<sup>25</sup> was used to describe the solvent effects in all calculations. The harmonic vibrational frequencies were computed and presented without scaling for the ground and lowest energy triplet excited states; the changes in the frequencies were compared with the experimental values obtained from TRIR spectroscopy. Mulliken and other charge analyses were performed for

different parts of the molecule, and consistent results were obtained (Table S4, Supporting Information). For brevity, only Mulliken charges are presented, and the results from other analyses are listed in the Supporting Information.

### 3. RESULTS

**Electrochemistry.** The redox properties of ReEB and ReEBA illustrate the significant differences among these complexes and the previously studied Re3DMABN associated with changing the diimine ligand from bpy to DCEB (Table 1).

**Table 1. Redox Potentials of ReEBA and Re3DMABN in DCM and CH<sub>3</sub>CN vs Ag/AgCl**

complex	$E^0(2+/+),$ ( $\Delta E_p$ , V) in DCM	$E^0(2+/+),$ ( $\Delta E_p$ , V) in CH <sub>3</sub> CN	$E^0(+/0),$ ( $\Delta E_p$ , V) in DCM	$E^0(+/0),$ ( $\Delta E_p$ , V) in CH <sub>3</sub> CN
Re3DMABN	1.28 (0.24)	1.17 (0.14)	−1.13	−1.17 (0.08)
ReEBA	1.15 (0.18)	1.17 (0.12)	−0.79	−0.78 (0.07)

The carboxyethyl substituents on the bpy ligand in DCEB lower the first one-electron reduction potential by 0.34 and 0.39 V in DCM and CH<sub>3</sub>CN, respectively, relative to the bpy complex. The potential of the first oxidation, reflecting the 3DMABN<sup>•+</sup>/3DMABN reduction, is altered only slightly upon changing the diimine ligand from bpy to DCEB. As was demonstrated elsewhere,<sup>26</sup> the diimine reduction potential decrease translates directly into a lowering of the MLCT state energy, as reflected in the luminescence maxima in both polar and nonpolar solvents.

**UV–vis Linear Absorption and Luminescence Spectra.** The absorption maximum at 335 nm for ReEBA in both DCM and NM is assigned to the DCEB ligand-localized  $\pi$ – $\pi^*$  transitions (Figure 1). The presence of the ester groups on the

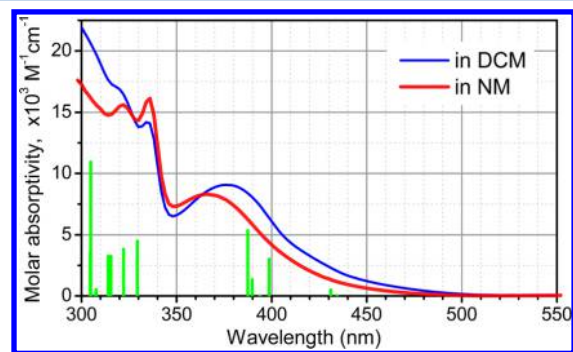


**Figure 1.** UV–vis absorption spectra of ReEBA in DCM and NM measured at 9 mM concentration in the sample cell with 50  $\mu$ m path length. Green bars show the calculated UV–vis absorption transitions using TD-DFT at Franck–Condon geometry.

DCEB ligand causes this transition to be red-shifted compared to the bpy-localized  $\pi$ – $\pi^*$  transitions in Re3DMABN (320 nm). The broad spectral features of ReEBA from 360 to 460 nm include a 3DMABN ligand-localized transition ( $\lambda_{\text{max}} = 370$  nm) and an MLCT state absorption as a weaker absorption that tails up to 460 nm.<sup>27–29</sup> Solvent polarity affects the strength of the transitions but does not induce major changes in their nature.

The complexes exhibit luminescence in nonpolar solvents at room temperature. Emission spectral maxima, quantum yields, lifetimes, and decay rate constants are given in Table 2. Luminescence from the DCEB complexes (ReEBA and ReEB)

is approximately 1100  $\text{cm}^{-1}$  lower in energy than in the corresponding bpy complex (Re3DMABN), increasing the likelihood that the MLCT state is lower in energy than the <sup>3</sup>IL state of the 3DMABN ligand (the observed excited state of Re3DMABN in DCM) in these complexes. The emission yield of ReEB is ca. 30% in DCM at room temperature, but the dimethylamino derivative ReEBA is only very weakly luminescent ( $\phi_{\text{lum}} = 0.003$ ), indicating a nonradiative process involving a dark state. Luminescence of the ReEB and ReEBA exhibits a significant red shift (800–1000  $\text{cm}^{-1}$ ) upon changing the solvent from DCM to mixed DCM/NM, illustrating that the MLCT state is stabilized in more polar solvents. The luminescence yield of the ReEBA complex becomes even weaker in the more polar solvent, suggesting that the energies of both the emitting and the dark state decrease with increasing solvent polarity.

**Vibrational Linear Absorption Spectra.** The vibrational spectrum of ReEBA (Figure 2) has several readily identifiable characteristic features (Table 3). The weak peak at ca. 2260  $\text{cm}^{-1}$  is the C $\equiv$ N stretching mode. The peaks at ca. 2043 and 1946  $\text{cm}^{-1}$  belong, respectively, to the symmetric and to two overlapping asymmetric stretching modes of the three facial carbonyl ligands. Another peak of interest at ca. 1735  $\text{cm}^{-1}$  belongs to two C=O stretching modes of the ester groups. No signature of splitting is found, suggesting that the coupling of the two carbonyl transitions is weak. Indeed, the closest possible distance between the two C=O transition dipoles is as large as 6.2 Å; moreover, for such a conformation, the angle between the transition dipoles is close to the magic angle, which results in a minimal splitting of the two coupled state energies. As assigned previously,<sup>14</sup> the ring stretching modes of the bpy,  $\nu_{\text{ss}}(\text{bpy})$ , and of the phenyl ring of 3DMABN,  $\nu_{\text{ss}}(\text{ph})$ , are also resolved in the spectra at 1610 and 1600  $\text{cm}^{-1}$ , respectively. While well resolved in the DCM solvent, in NM, they overlap with a strong solvent absorption around 1600  $\text{cm}^{-1}$ . All of these modes were used in transient infrared measurements as reporters of the changes in the electron-density distribution in the compounds.

**Transient Infrared Spectroscopy.** TRIR spectra were measured from 1480 to 2300  $\text{cm}^{-1}$  to cover the spectral region of the C $\equiv$ N (2120–2300  $\text{cm}^{-1}$ ), C $\equiv$ O (1800–2120  $\text{cm}^{-1}$ ), C=O (1640–1800  $\text{cm}^{-1}$ ), and ring (1480–1620  $\text{cm}^{-1}$ ) modes (Figure 3). The transient spectra represent the difference between the vibrational spectra in the excited and ground electronic states; positive peaks occur due to absorption of modes in the excited states, and negative peaks are due to bleaching of the modes in the ground electronic state. Each vibrational mode indicated above is localized on a specific moiety (ligand) of the complex and therefore reports on changes in electron density at the respective moiety; DFT calculations on the complexes, including solvent polarization effects, support the idea of mode localization. Analysis of all of the available spectral features is essential for a consistent assignment of the excited-state character.

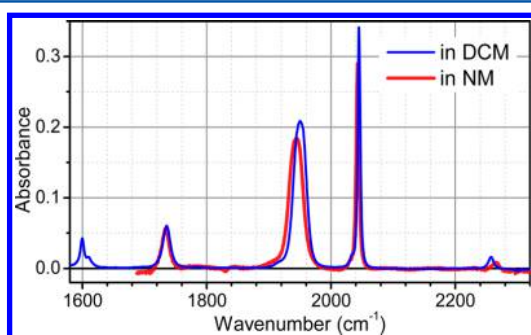
**MLCT State Formation.** All ReEBA characteristic mode frequencies change upon 402 nm excitation. The initial spectral changes, assigned to formation of the Re to bpy MLCT state, are essentially instantaneous within the time resolution of ca. 200 fs. The  $\nu(\text{C}\equiv\text{N})$  peak decreases in frequency by 15  $\text{cm}^{-1}$ , and its transition dipole increases by more than a factor of 10 in the excited state (Figure 3). The shift and intensity increase are similar to those observed in the Re3DMABN and Re4DMABN



**Table 2. Luminescence Maximum ( $\lambda_{\text{max}}$ ), Quantum Yield ( $QY_{\text{lum}}$ ), and the Excited State Lifetimes Measured via Luminescence ( $T_{\text{lum}}$ ) and Transient Absorption ( $T_1$ ) for the Complexes in Aerated Solvents at Room Temperature<sup>a</sup>**

complex	Re3DMABN		ReEB		ReEBA	
solvent	DCM	DCM/MeOH	DCM	DCM/NM <sup>d</sup>	DCM	DCM/NM
$\lambda_{\text{max}}$ (nm)	528	565	566	586	562	584
$QY_{\text{lum}}$	0.003	<0.001	0.26	0.09	0.003 <sup>e</sup>	<<0.0001
$T_{\text{lum}}$ ( $\mu\text{s}$ )	31 <sup>b</sup>		0.94 $\pm$ 0.02	0.47 $\pm$ 0.02	0.04 $\pm$ 0.005 <sup>c</sup>	
$T_1$ ( $\mu\text{s}$ ) ( $\lambda$ , nm) <sup>c</sup>	23.3 $\pm$ 1.0 (450)	0.02 $\pm$ 0.005 (450)	0.91 $\pm$ 0.02 (350)	0.44 $\pm$ 0.02 (480)	0.05 $\pm$ 0.01 (480)	
$k_r$ ( $\text{s}^{-1}$ )	130		2.8 $\times 10^5$	2.0 $\times 10^5$		
$k_{\text{nr}}$ ( $\text{s}^{-1}$ )	5.0 $\times 10^4$		8 $\times 10^5$	2.1 $\times 10^6$		

<sup>a</sup>The radiative ( $k_r$ ) and nonradiative ( $k_{\text{nr}}$ ) relaxation constants are also shown. <sup>b</sup>The mean value of two components is shown. <sup>c</sup>The lifetime measured by transient absorption at indicated wavelengths. <sup>d</sup>A 1:1 (v/v) mixture of DCM and NM was used. <sup>e</sup>A second emission component is observed with a lifetime of  $\sim 800$  ns; this is believed to be due to an impurity Re complex.

**Figure 2.** Linear FTIR absorption spectra of ReEBA in DCM and NM measured at 9 mM concentration in the sample cell with 50  $\mu\text{m}$  path length.

compounds,<sup>14</sup> also assigned to formation of an MLCT (Re  $\rightarrow$  bpy) state.

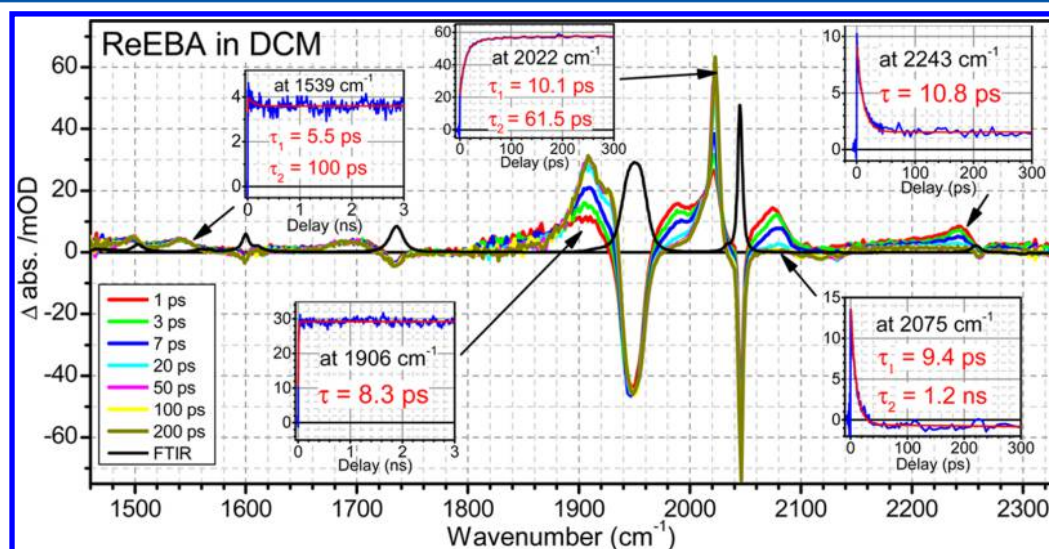
The C $\equiv$ O stretching modes are known to be useful probes of changes to the metal center charge because the  $\pi$  backbonding from the metal to the C $\equiv$ O is strongly influenced by the metal's charge.<sup>15,16</sup> An increase in the positive charge on Re will cause an upshift in the  $\nu(\text{C}\equiv\text{O})$  frequencies. The frequency upshift values, 74 (as1), 42 (as2), and 28  $\text{cm}^{-1}$  (ss), are larger than those for Re3DMABN in DCM in its MLCT state, which are 70 (as1), 30 (as2), and 17  $\text{cm}^{-1}$  (ss). This indicates that the MLCT state formed features more positive

**Table 3. Experimental and DFT Computed Ground-State Vibrational Frequencies (in  $\text{cm}^{-1}$ ) of Several Characteristic Modes for ReEBA in Both DCM and NM**

ReEBA in DCM		ReEBA in NM		Assignment
Exper.	DFT, GS	Exper.	DFT, GS	
2258	2341	2266	2343	$\nu(\text{C}\equiv\text{N})$
2046	2106	2043	2104	$\nu_{\text{ss}}(\text{C}\equiv\text{O})$
1949	2009	1945	2007	$\nu_{\text{as}}(\text{CO}) \begin{cases} \text{as}_1 \\ \text{as}_2 \end{cases}$
	2003		2000	
1735	1789	1734	1786	$\nu_{\text{ss}}(\text{C}=\text{O})$
1735	1788	1734	1786	$\nu_{\text{as}}(\text{C}=\text{O})$
1610	1612/1604	N/A	1613/1605	$\nu_{\text{ss}}(\text{bpy})$
1600	1646	N/A	1646	$\nu_{\text{ss}}(\text{Ph})$

charge on Re. The two  $\nu_{\text{as}}(\text{C}\equiv\text{O})$  modes that overlap in the ground state are resolved in the excited state (Table 4), indicating a decreased symmetry among the environment for the three carbonyl ligands. Note that the reduction of electron density at the metal causes an upshift in the C $\equiv$ O frequencies but a downshift in the C $\equiv$ N frequency. This is because the antibonding orbitals of the nitrile group have much higher energies than those in the carbonyls, preventing their population through the metal center.<sup>30</sup>

The C=O modes of the ester groups are expected to be good reporters of the DCEB ligand charge changes. The C=O modes in the MLCT state absorb at ca. 1694  $\text{cm}^{-1}$ , which is ca. 39  $\text{cm}^{-1}$  lower than their ground state frequency.

**Figure 3.** Transient infrared spectrum of ReEBA in DCM following 402 nm excitation at selected time delays. Insets show kinetics measured at indicated frequencies and their fits to single or double exponential functions.

**Table 4.** Experimental Frequency Shifts (in  $\text{cm}^{-1}$ ) for Indicated Vibrational Modes of ReEBA and Re3DMABN in the  $^3\text{MLCT}$  State vs the Ground State ( $\Delta_1$ ) and in the Long-Lived Excited State<sup>a</sup> vs the Ground State ( $\Delta_2$ )

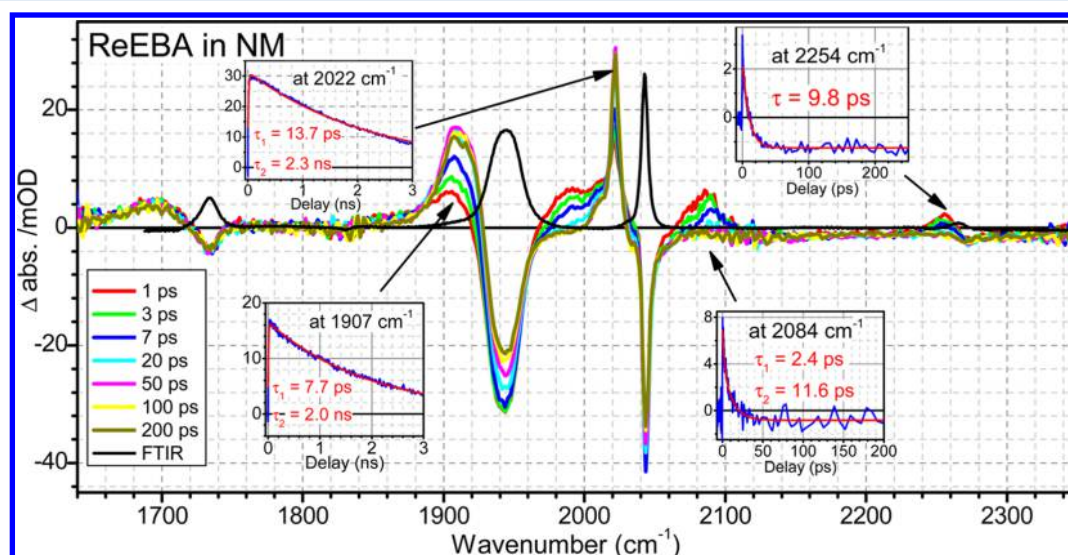
	solvent	$\nu_{\text{as}2}(\text{C}\equiv\text{O})$		$\nu_{\text{as}1}(\text{C}\equiv\text{O})$		$\nu_{\text{ss}}(\text{C}\equiv\text{O})$		$\nu(\text{C}\equiv\text{N})$		$\nu(\text{C}=\text{O})$	
		$\Delta_1$	$\Delta_2$	$\Delta_1$	$\Delta_2$	$\Delta_1$	$\Delta_2$	$\Delta_1$	$\Delta_2$	$\Delta_1$	$\Delta_2$
ReEBA	DCM	+42	-21	+74	-39	+28	-24	-15	N/A	-39	-39
ReEBA	NM	+47	-28	+78	-35	+42	-23	-10	N/A	-38	-38
Re3DMABN	DCM	+34	-59	+70	-96	+14	-29	-12	-118	N/A	N/A
Re3DMABN	DCM/MeOH	+33	+3.5	+70	+3	+24	+10	-12	-123	N/A	N/A
ReBN	DCM	+30	+6	+64	+5	+11	+2.5	-10.5	0	N/A	N/A

<sup>a</sup>The nature of the long-lived excited state is different for different compounds (see text).

**Table 5.** Experimental and Calculated Frequency Differences between the Ground State and Lowest Energy Excited State

	solvent		$\nu_{\text{as}2}(\text{C}\equiv\text{O})$	$\nu_{\text{as}1}(\text{C}\equiv\text{O})$	$\nu_{\text{ss}}(\text{C}\equiv\text{O})$	$\nu(\text{C}\equiv\text{N})$	$\nu(\text{C}=\text{O})$	$\nu(\text{bpy})$
ReEBA	DCM	exptl	-21	-39	-24	N/A	-39	-60
		calcd	-10	-22	-24	+13 <sup>a</sup>	-31	-36/-60
ReEBA	NM	exptl	-28	-35	-23	N/A	-38	N/A
		calcd	-21	-28	-23	+15 <sup>a</sup>	-34	-40/-63

<sup>a</sup>The DFT computed IR intensity in the excited state is more than 3 times weaker than that in the ground state.

**Figure 4.** Transient infrared spectrum of ReEBA in NM following 402 nm excitation at selected time delays. Insets show kinetics measured at indicated frequencies and their fits to a single or double exponential function.

The  $\nu(\text{C}=\text{O})$  peak in the excited state is much broader and has a higher IR intensity than that in the ground state, which suggests that the DCEB ligand is more highly charged in the excited state. The broader spectrum may be a result of a larger splitting of the two carbonyl transitions that bear a larger IR intensity in the excited state.

Two ring stretching modes,  $\nu(\text{bpy})$  and  $\nu(\text{ph})$ , also undergo changes in the excited state, most notably by the appearance of a broad peak at  $1540\text{ cm}^{-1}$ . Because of the closeness of the  $\nu(\text{bpy})$  and  $\nu(\text{ph})$  peaks in the ground state, this excited-state peak can originate from either of the two modes. The DFT calculations of the triplet excited state showed two vibrational modes with high IR intensity in this region, and both of them belong to the ring stretching modes of the bpy moiety. The two  $\nu(\text{bpy})$  modes, which feature  $-38$  and  $-61\text{ cm}^{-1}$  downshifts with respect to the ground state, appear as a broad peak at  $1540\text{ cm}^{-1}$ . Such a large downshift is caused by electron transfer from Re to the DCEB ligand in the MLCT state. This peak at  $1540\text{ cm}^{-1}$  undergoes narrowing and intensity growth with a characteristic time of ca. 5.5 ps, which is typical for the

solvation process in DCM. Similar to that reported previously for Re3DMABN,<sup>14</sup> the  $\nu(\text{ph})$  peak at  $1600\text{ cm}^{-1}$  is shifted by ca. 3–5  $\text{cm}^{-1}$  to smaller frequencies, as indicated by canceled bleaching at ca.  $1593\text{ cm}^{-1}$  in the 1–7 ps-delay spectra.

#### MLCT State Decay and Formation of an LLCT State.

The transient IR spectra of ReEBA show large changes with a characteristic time of ca. 10 ps, which do not lead to recovery of the ground state bleach features, thus indicating formation of a new excited state. Because the state formed for ReEBA in DCM with the 10 ps time constant is long-lived (no decay in the 3 ns time window, see Figure 3 insets), its experimental features are compared to the features of the lowest-energy triplet state, computed using the variational approach (Table 5).

The cyano group absorption decays to a weak and broad feature but not to zero, indicating a large reduction in the IR intensity. DFT calculations indicate that  $\nu(\text{C}\equiv\text{N})$  of the lowest energy triplet state is ca. 3-fold weaker than that in the ground state (Table 5), while its frequency is ca. 13  $\text{cm}^{-1}$  higher than that in the ground state. The DFT calculations indicate that the lowest energy triplet state has LLCT character.

The C≡O peaks in the MLCT state found at ca. 1990 and 2070 cm<sup>-1</sup> decay to the baseline with a characteristic time of 10 ps, indicating a complete depletion of the MLCT state. Concomitant with the decay, the C≡O peaks at ca. 1908, 1926, and 2022 cm<sup>-1</sup> grow in. The C≡O frequencies in this state appear lower than those in the ground state by 39, 21, and 24 cm<sup>-1</sup>, which match well the computed shifts for the lowest excited triplet state (34, 22, and 28 cm<sup>-1</sup>, Table 5). Large shifts to smaller frequencies for all three  $\nu(\text{C}\equiv\text{O})$  modes suggest accumulation of an additional negative charge at the Re center. Such charge redistribution is expected if an electron is transferred from the amino group of 3DMABN to Re and the DCEB ligand.

The C=O absorption peak in the MLCT state at 1695 cm<sup>-1</sup> does not show much frequency shift with time, but its amplitude increases by about 12% with a 10 ps time constant. This suggests that the charge on the DCEB ligand changes little in the LLCT state compared to that in the MLCT state. The DFT computations predict a 33 cm<sup>-1</sup> downshift for the C=O mode frequencies and ca. 2-fold increase of their IR intensities, which reproduce the experimental observations. The excited-state C=O peak does not show any decay within the probed time window of ca. 3 ns; the excited-state lifetime of 43 ns was obtained via ns transient UV–vis absorption.

The  $\nu(\text{bpy})$  ring modes in the LLCT state show similar behavior to that of the C=O modes: the intensity growth here is accompanied by peak narrowing, which occurs with a characteristic time of ca. 5.5 ps and is assigned to the solvation process in DCM and vibrational cooling.<sup>16,31–33</sup> A small 100 ps component may reflect structural rearrangements; similar components were previously observed in other Re complexes.<sup>14</sup>

**Solvent Effects.** The TRIR spectra of ReEBA measured in solvents of different polarities, i.e., less polar DCM (Figure 3) and more polar nitromethane (NM, Figure 4), were compared. Due to solvent absorption, no spectra were recorded below 1650 cm<sup>-1</sup> in NM. Although the spectral features of ReEBA in NM are similar to those in DCM and a similar MLCT state conversion to LLCT state was observed with a similar time constant of ca. 10 ps, several differences are noteworthy. First, the lifetime of the LLCT state in NM (2.4 ns) is much shorter than that in DCM (43 ns). In addition, compared to that in DCM, there are larger upshifts of the three C≡O peaks in the MLCT state in NM and the absence of an additional rise with time in the C=O absorption in NM at ca. 1690 cm<sup>-1</sup> following initial MLCT state formation. These observations point to the same effect, namely, that a larger positive charge is formed at Re in the MLCT state in NM and a larger negative charge is formed at DCEB upon MLCT state formation. Similar C≡O peak dependences were observed for Re3DMABN and Re4DMABN compounds when switching the solvent from DCM to DCM/MeOH mixture.<sup>14</sup>

#### 4. DISCUSSION

The experimental and computational data described here allow us to track the changes in the electron density between the ground and excited states of the ReEBA complex. As the solvent polarity does not strongly affect the MLCT to LLCT processes, we focus on the data for ReEBA in DCM below.

Formation of the  $\text{Re}(\text{d}\pi) \rightarrow \text{DCEB}(\pi^*)$  MLCT state is apparent from the TRIR data. The C≡O modes alone are sufficient to conclude that the upshift of all three C≡O mode frequencies is characteristic of establishing increased positive charge at the metal. The frequency shifts are uniformly larger

than those observed previously in Re3DMABN and ReBN compounds (Table 4),<sup>14</sup> suggesting that a larger amount of charge is transferred from the metal. Formation of the MLCT state is faster than our time resolution of ca. 200 fs due to a strong spin–orbit coupling at the Re atom. A considerable number of reports indicate that the electronic relaxation time to form a triplet MLCT state for Re complexes is a few hundred femtoseconds.<sup>13,20</sup> Other vibrational modes in the complex also report the formation of the MLCT state. For example, the downshift of the  $\nu(\text{C}\equiv\text{N})$  frequency by 15 cm<sup>-1</sup> is similar to that for ReBN (–10.5 cm<sup>-1</sup>) and Re3DMABN (–12 cm<sup>-1</sup>).<sup>14</sup> The amount of charge transferred from the metal to the ligand varies for different complexes. It is expected that the amount of charge transfer increases from Re3DMABN to ReEBA in accord with a decrease in the reduction potential for the electron accepting ligand (Table 1).

The lowest energy triplet excited state of ReEB is the MLCT state, which can serve to characterize the amount of charge transferred in the MLCT state for ReEBA and to correlate the charge transfer to the frequency shifts of vibrational labels in the DCEB ligand. The DFT computation of the lowest energy triplet in ReEB predicts that ca. 0.54 electron charge is transferred to the DCEB ligand in the MLCT state.

The MLCT state relaxes rapidly (10 ps) into another state that is assigned as an LLCT state. The  $\nu(\text{C}\equiv\text{O})$  frequency shifts indicate the formation of a negative charge on the metal compared to that in the GS, although the assignment of the state formed as LLCT is less unambiguous based on  $\nu(\text{C}\equiv\text{O})$  peaks alone, as the <sup>3</sup>IL state at 3DMABN is also characterized by a downshift of the  $\nu(\text{C}\equiv\text{O})$  frequencies.<sup>14</sup> Combined use of all measured IR reporters provides a clear picture for the state assignment. In particular, the  $\nu(\text{C}\equiv\text{N})$  mode is instrumental in distinguishing the LLCT and <sup>3</sup>IL states, as it shifts to smaller frequencies by ca. 120 cm<sup>-1</sup> in the latter. Thus, a large frequency shift of  $\nu(\text{C}\equiv\text{N})$  in the <sup>3</sup>IL state results from the electron density shift from the dimethyl amino moiety and phenyl ring to the CN group.<sup>14,34</sup> A lack of  $\nu(\text{C}\equiv\text{N})$  peak shift to the ca. 2130 cm<sup>-1</sup> region indicates that electron density changes do not involve the CN group, signifying that formation of the <sup>3</sup>IL state is not occurring in ReEBA. The C=O modes at 1735 cm<sup>-1</sup> serve as reporters of the DCEB ligand charge redistribution. After its initial downshift of 36 cm<sup>-1</sup> in the MLCT state, the excited-state C=O modes show no further shift and only a small increase (less than 20%) in the IR intensity with a characteristic time of 10 ps following the instantaneous rise of the peak. The DFT calculations predict a 33 cm<sup>-1</sup> frequency downshift of  $\nu(\text{C}\equiv\text{O})$  in the lowest energy excited state, which matches the experimental value well; this downshift corresponds to an increase in the negative charge on the DCEB ligand. Thus, with formation of the MLCT state, the DCEB moiety receives a large amount of negative charge from the Re atom. The amount of negative charge at DCEB increases further with formation of the LLCT state, and now the electron density is transferred from the 3DMABN ligand (Figure 5).

MLCT state	LLCT state
-0.54 0.49 0.05	-0.82 -0.10 0.92
DCEB–Re–3DMABN (CO) <sub>3</sub>	DCEB–Re–3DMABN (CO) <sub>3</sub>

**Figure 5.** Changes in Mulliken charges at different moieties of ReEBA in <sup>3</sup>MLCT and LLCT states vs the ground state. Notice that the charge changes given for the MLCT state were computed for the lowest excited triplet state for ReEB in DCM.



The same picture is reported by the bpy ring stretching mode peak; the peak at  $1539\text{ cm}^{-1}$  is formed in the MLCT state and shows only a minor amplitude increase and narrowing with the MLCT  $\rightarrow$  LLCT conversion.

The combined electrochemical and luminescence data are also consistent with the relative populations of the MLCT and ILCT states described above. The energy of the long-lived excited state for ReEBA in DCM is approximately 2.2 eV, based on the luminescence maximum. The energy of the LLCT state can be approximated from the difference in the potential between the coordinated 3DMABN $^{+*}$ /3DMABN reduction and the coordinated DECB ligand, which is 1.94 V in DCM. Thus, the MLCT state is about 0.25 V higher in energy than the LLCT state, and there is less than 0.1% MLCT state present at equilibrium. The same analysis in the more polar solvent indicates that the MLCT state is approximately 0.15 V higher in energy than the LLCT state, still leaving excited less than 1% of the MLCT state in an equilibrium of the two states. The results are consistent with the transient IR data that show complete disappearance of the MLCT state and the extremely weak luminescence observed from ReEBA in both DCM and DCM/NM. Thus, given this equilibrium model, it is reasonable to assign this luminescence as originating from an MLCT state rather than the predominant LLCT state.

The excited-state lifetime of the lowest-energy state of ReEBA in DCM solvent was obtained using nanosecond transient absorption spectroscopy. The excited-state lifetime measured for ReEBA is 43 ns, which is ca. 3 orders of magnitude smaller than that for Re3DMABN (23  $\mu$ s) in the same solvent, DCM. The large reduction in the lifetime of ReEBA also indicates that the lowest energy state differs from Re3DMABN (which is  $^3\text{IL}$ ). A substantial solvent dependence of the lifetime further supports the assignment: the lifetime reduces from 43 ns in DCM to 2.4 ns in NM. The large influence of solvent polarity on the excited-state relaxation process in ReEBA indicates that the excited state is strongly polarized, suggesting that it has a LLCT character. As stated above, the energy of the charge separated state is greater than 1.9 eV in both solvents and differs by only 10 mV between the two solvents. In addition, the rigidity of the participating electron donor and acceptor in ReEBA suggests that the inner sphere reorganization energy for recombination is unlikely to differ significantly between the two solvents. The observed change in the charge recombination rate is therefore most likely linked to differences in the solvent reorganization energy. A dielectric continuum picture of solvent reorganization ( $\lambda_s$ ) would dictate that  $\lambda_s$  is larger for NM than for DCM and therefore back electron transfer in DCM is probably in the Marcus inverted region.

Excited state characterization of ReEBA using DFT calculations supports the interpretation of the experiments. The frequency difference of all examined vibrational modes was calculated, and very good agreement was found between the experimental and DFT data (Table 5). To quantify the changes in the electron density in different regions of the complex between different excited states, Mulliken charge analysis was used (Table 6). A charge of 0.92 electrons is computed to be transferred from the 3DMABN ligand to the rest of the molecule, mostly to the DCEB ligand (Table 6) in the DFT analysis.

To assess the amount of charge transferred between the ligands in the LLCT state, the C $\equiv$ O peak frequency shifts can be compared to those reported for fully reduced compounds

**Table 6. Computed Mulliken Charges at Different Moieties of the ReEBA and ReEB Compounds for the Ground State (S0) and the Lowest Energy Triplet Excited State (T1) in DCM and in NM and the Charge Changes (T1–S0)<sup>a</sup>**

	S0	T1	T1–S0
ReEBA in DCM			
Re(CO) <sub>3</sub>	0.31	0.21	–0.10
DCEB	0.49	–0.33	–0.82
3DMABN	0.20	1.12	0.92
ReEBA in NM			
Re(CO) <sub>3</sub>	0.30	0.19	–0.11
DCEB	0.49	–0.34	–0.83
3DMABN	0.21	1.15	0.94
ReEB in DCM			
Re(CO) <sub>3</sub>	0.31	0.8	0.49
DCEB	0.50	–0.04	–0.54
PhCN	0.19	0.24	0.05
ReEB in NM			
Re(CO) <sub>3</sub>	0.31	0.82	0.51
DCEB	0.50	–0.06	–0.56
PhCN	0.19	0.24	0.05

<sup>a</sup>Table S4 (Supporting Information) gives charge density changes computed using three other approaches: Lowdin, ESP, and NBO.

with similar structure. A [Re(CO)<sub>3</sub>Cl(dcbpy)] complex, where dcbpy is 4,4'-dicarboxy-2,2'-bipyridine, attached to a CdSe quantum dot via a carboxylate group was studied by Lian and co-workers.<sup>35</sup> Electron injection from the quantum dot to the complex was observed upon electronic excitation. The complex reduction, with the electron residing on the dcbpy ligand, was accompanied by a downshift of the C $\equiv$ O frequencies. The values of the downshift, 18, 32, and 22  $\text{cm}^{-1}$  for  $\nu_{\text{as1}}(\text{C}\equiv\text{O})$ ,  $\nu_{\text{as2}}(\text{C}\equiv\text{O})$ , and  $\nu_{\text{ss}}(\text{C}\equiv\text{O})$ , respectively, resemble closely the values found for ReEBA in the LLCT state (Table 4). Grills and co-workers prepared reduced [Re(bpy)(CO)<sub>3</sub>(CH<sub>3</sub>CN)] species in water using pulse radiolysis.<sup>36</sup> The C $\equiv$ O frequency shifts due to the reduction, 26  $\text{cm}^{-1}$  for  $\nu_{\text{ss}}(\text{C}\equiv\text{O})$  and 32  $\text{cm}^{-1}$  for  $\nu_{\text{as}}(\text{C}\equiv\text{O})$ , are again very similar to those observed in this study for the LLCT state. There is also a considerable amount of spectroelectrochemistry data for rhenium tricarbonyl diimine complexes in the literature, where the  $\nu(\text{C}\equiv\text{O})$  frequencies in the reduced complexes were measured. The one-electron reduced species show a shift of the  $\nu_{\text{ss}}(\text{C}\equiv\text{O})$  peak by ca. 27  $\text{cm}^{-1}$ .<sup>37–40</sup> This value also matches well the  $\nu_{\text{ss}}(\text{C}\equiv\text{O})$  frequency shift observed for ReEBA (24  $\text{cm}^{-1}$ ), supporting the assignment of its lowest energy excited state as the LLCT state, featuring a nearly full-electron transfer from the 3DMABN ligand to the DCEB ligand. Thus, a range of data reported in the literature is in agreement with the assessment that the LLCT state in ReEBA features charge separation exceeding 0.9 electron charge.

The nature of the LLCT state of ReEBA can be understood well by using a previously developed three-state coupling model (Figure 6).<sup>14</sup> In this model, three electronic states were assumed: a pure MLCT (Re  $\rightarrow$  bpy or DCEB) state, a full-electron CT (L  $\rightarrow$  bpy or DCEB) state, and an ideal triplet ( $^3\text{IL}$ ) state fully localized on the L ligand. Mixing of these three states results in the formation of the characteristic states of the complex. The  $^3\text{IL}$  state is weakly coupled to the other two states.<sup>14</sup> The pure MLCT state and full-electron CT state are coupled, as both states feature electron transfer to bpy or DCEB; the coupling strength is determined by the spatial



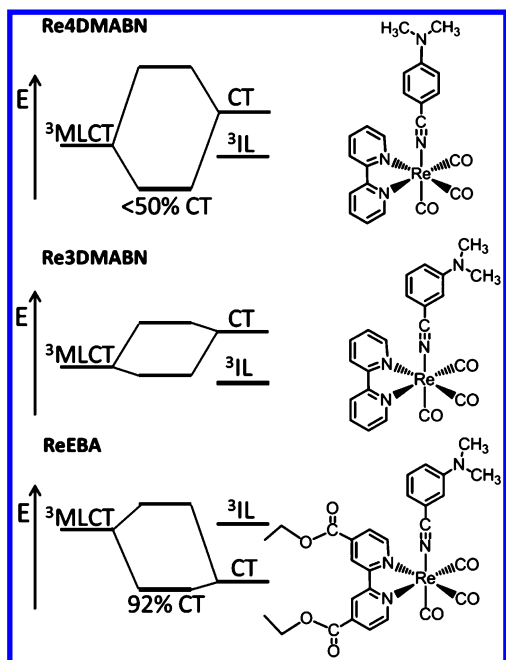


**Figure 6.** A three-state model describing the charge-transfer extent in Re4DMABN, Re3DMABN, and ReEBA in the DCM solvent.

overlap of the wave functions for the two ideal states. This coupling is very strong in Re4DMABN because of the quinoidal resonant structure on the 4DMABN ligand. As a result, the mixed state is lowered in energy substantially but has a significant contribution from both MLCT and CT states. The MLCT and CT state coupling in Re3DMABN is much weaker compared to that in Re4DMABN, due to a lack of quinoidal resonant structure, resulting in a smaller shift of the mixed state energies (Figure 6). Consequently, the  $^3\text{IL}$  state of 3DMABN is the lowest energy state in Re3DMABN in DCM. By placing two electron-withdrawing carboxyethyl groups on the bpy ligand, the MLCT and CT state energies of ReEBA were lowered with respect to those for Re3DMABN, as DCEB is a stronger electron acceptor than bpy. Note that the CT state energy was lowered more dramatically than the MLCT state, as the CT state features a larger charge separation distance. An increased energy gap between the MLCT and CT states, together with their weak mixing, facilitates formation of the mixed LLCT state that has mostly CT character. Indeed, the overall experimental and computational results indicate that the lowest energy state for ReEBA is characterized by ca. 92% LLCT character.

## 5. CONCLUSIONS

The excited-state dynamics of ReEBA and ReEB were studied in DCM and NM solvents using time-resolved infrared and electronic spectroscopy and DFT analysis. The lowest energy excited state of ReEBA was assigned to a full-electron (3DMABN  $\rightarrow$  DCEB) LLCT state, on the basis of experimental and computational data summarized here: (1) The luminescence quantum yield of ReEBA is 2 orders of magnitude smaller than that in ReEB, indicating that the MLCT state luminescence is quenched by formation of the LLCT state. The lifetime of the lowest energy excited state of ReEBA decreases dramatically with an increase in solvent polarity, which is indicative of forming a strongly polarized state. (2) Characteristic changes in the vibrational frequencies of the excited state, including a large down shift of the  $\text{C}\equiv\text{O}$

modes, the absence of a  $\text{C}\equiv\text{N}$   $^3\text{IL}$  state peak at ca.  $2130\text{ cm}^{-1}$ , and changes of  $\nu(\text{C}=\text{O})$  and  $\nu(\text{bpy})$  modes, agree well with the formation of the LLCT state. (3) DFT calculations predict that the amount of charge transferred from the 3DMABN ligand, largely to the DCEB ligand, in the lowest energy excited state is ca. 0.92 of electron charge. Note that formation of a nearly pure LLCT state (about 92%) was accomplished by tuning the redox properties of the electron accepting ligand (DCEB) and simultaneously decoupling the redox active group of the electron donating ligand (3DMABN) from the metal. This molecular engineering strategy permits the design of compact transition metal complexes that feature excited states with essentially full-electron LLCT states.

## ■ ASSOCIATED CONTENT

### Supporting Information

A detailed description of the synthesis of the compounds,  $^1\text{H}$  NMR spectra, MALDI mass spectra, cyclic voltammetry, nanosecond transient absorption data, and computational data is presented. This material is available free of charge via the Internet at <http://pubs.acs.org>.

## ■ AUTHOR INFORMATION

### Corresponding Author

\*E-mail: [irubtsov@tulane.edu](mailto:irubtsov@tulane.edu).

### Notes

The authors declare no competing financial interest.

## ■ ACKNOWLEDGMENTS

Support by the National Science Foundation (CHE-012357 to D.N.B. and CHE-1012371 to I.V.R.) and the U.S. Department of Energy, Office of Chemical Sciences (DE-FG-02-96ER14617 to R.H.S.) is gratefully acknowledged. The Louisiana Board of Regents (Grant LEQSF(2011-12)-ENH-TR-29) is thanked for supporting acquisition of the fs Ti:sapphire laser system. T.G. wishes to thank the Louisiana Board of Regents for Graduate Fellowship support. Y.Y. is thankful for a fellowship from the IBM Corporation.

## ■ REFERENCES

- (1) Wenger, O. S. How Donor-Bridge-Acceptor Energetics Influence Electron Tunneling Dynamics and Their Distance Dependences. *Acc. Chem. Res.* **2011**, *44*, 25–35.
- (2) Wenger, O. S. Barrier Heights in Long-Range Electron Tunneling. *Inorg. Chim. Acta* **2011**, *374*, 3–9.
- (3) Kirk, M. L.; Shultz, D. A. Transition Metal Complexes of Donor–Acceptor Biradicals. *Coord. Chem. Rev.* **2013**, *257*, 218–233.
- (4) Skourtis, S. S.; Waldeck, D. H.; Beratan, D. N. Inelastic Electron Tunneling Erases Coupling-Pathway Interferences. *J. Phys. Chem. B* **2004**, *108*, 15511–15518.
- (5) Skourtis, S. S.; Waldeck, D. H.; Beratan, D. N. Fluctuations in Biological and Bioinspired Electron-Transfer Reactions. *Annu. Rev. Phys. Chem.* **2010**, *61*, 461–485.
- (6) Lin, Z.; Lawrence, C. M.; Xiao, D.; Kireev, V. V.; Skourtis, S. S.; Sessler, J. L.; Beratan, D. N.; Rubtsov, I. V. Modulating Unimolecular Charge Transfer by Exciting Bridge Vibrations. *J. Am. Chem. Soc.* **2009**, *131*, 18060–18062.
- (7) Verma, S.; Kar, P.; Das, A.; Ghosh, H. N. Photophysical Properties of Ligand Localized Excited State in Ruthenium(II) Polypyridyl Complexes: A Combined Effect of Electron Donor–Acceptor Ligand. *Dalton Trans.* **2011**, *40*, 9765–9773.
- (8) Lewis, J. D.; Towrie, M.; Moore, J. N. Ground- and Excited-State Infrared Spectra of an Azacrown-Substituted  $[(\text{bpy})\text{Re}(\text{CO})_3\text{L}]^+$

Complex: Structure and Bonding in Ground and Excited States and Effects of  $\text{Ba}^{2+}$  Binding. *J. Phys. Chem. A* **2008**, *112*, 3852–3864.

(9) Busby, M.; Gabrielson, A.; Matousek, P.; Towrie, M.; Di Bilio, A. J.; Gray, H. B.; Vlcek, A., Jr. Excited-State Dynamics of *fac*- $[\text{Re}^{\text{I}}(\text{L})(\text{CO})_3(\text{phen})]^+$  and *fac*- $[\text{Re}^{\text{I}}(\text{L})(\text{CO})_3(5\text{-NO}_2\text{-phen})]^+$  (L = imidazole, 4-ethylpyridine; phen = 1,10-phenanthroline) Complexes. *Inorg. Chem.* **2004**, *43*, 4994–5002.

(10) Meyer, T. J. Intramolecular Control of Excited State Electron and Energy Transfer. *Pure Appl. Chem.* **1990**, *62*, 1003–1009.

(11) Bernhard, S.; Omberg, K. M.; Strouse, G. F.; Schoonover, J. R. Time-Resolved IR Studies of  $\text{Re}(\text{LL})(\text{CO})_4]^+$ . *Inorg. Chem.* **2000**, *39*, 3107–3110.

(12) Omberg, K. M.; Schoonover, J. R.; Bernhard, S.; Moss, J. A.; Treadway, J. A.; Kober, E. M.; Dyer, R. B.; Meyer, T. J. Mid-Infrared Spectrum of  $[\text{Ru}(\text{phen})_3]^{2+}$ . *Inorg. Chem.* **1998**, *37*, 3505–3508.

(13) Cannizzo, A.; Blanco-Rodriguez, A. M.; El Nahhas, A.; Sebera, J.; Zalis, S.; Vlcek, A., Jr.; Chergui, M. Femtosecond Fluorescence and Intersystem Crossing in Rhenium(I) Carbonyl-Bipyridine Complexes. *J. Am. Chem. Soc.* **2008**, *130*, 8967–8974.

(14) Yue, Y.; Grusenmeyer, T.; Ma, Z.; Zhang, P.; Pham, T. T.; Mague, J. T.; Donahue, J. P.; Schmehl, R. H.; Beratan, D. N.; Rubtsov, I. V. Evaluating the Extent of Intramolecular Charge Transfer in the Excited States of Rhenium(I) Donor-Acceptor Complexes with Time-Resolved Vibrational Spectroscopy. *J. Phys. Chem. B* **2013**, *117*, 15903–15916.

(15) Kleverlaan, C. J.; Stufkens, D. J.; Clark, I. P.; George, M. W.; Turner, J. J.; Martino, D. M.; van Willigen, H.; Vlcek, A. Photoinduced Radical Formation from the Complexes  $[\text{Re}(\text{R})(\text{CO})_3(4,4'\text{-Me}_2\text{-bpy})]$  (R =  $\text{CH}_3$ ,  $\text{CD}_3$ , Et,  $^i\text{Pr}$ , Bz): A Nanosecond Time-Resolved Emission, UV–Vis and IR Absorption, and FT-EPR Study. *J. Am. Chem. Soc.* **1998**, *120*, 10871–10879.

(16) Liard, D. J.; Busby, M.; Matousek, P.; Towrie, M.; Vlcek, A. Picosecond Relaxation of  $^3\text{MLCT}$  Excited States of  $[\text{Re}(\text{Etpy})-(\text{CO})_3(\text{dmb})]^+$  and  $[\text{Re}(\text{Cl})(\text{CO})_3(\text{bpy})]$  as Revealed by Time-Resolved Resonance Raman, UV–vis, and IR Absorption Spectroscopy. *J. Phys. Chem. A* **2004**, *108*, 2363–2369.

(17) Dattelbaum, D. M.; Omberg, K. M.; Hay, P. J.; Gebhart, N. L.; Martin, R. L.; Schoonover, J. R.; Meyer, T. J. Defining Electronic Excited States Using Time-Resolved Infrared Spectroscopy and Density Functional Theory Calculations. *J. Phys. Chem. A* **2004**, *108*, 3527–3536.

(18) Blanco-Rodriguez, A. M.; Kvapilova, H.; Sykora, J.; Towrie, M.; Nervi, C.; Volpi, G.; Zalis, S.; Vlcek, A., Jr. Photophysics of Singlet and Triplet Intraligand Excited States in  $[\text{ReCl}(\text{CO})_3(1\text{-(2-pyridyl)-imidazo}[1,5\text{-}\alpha]\text{pyridine})]$  Complexes. *J. Am. Chem. Soc.* **2014**, *136*, 5963–5973.

(19) Vlcek, A.; Busby, M. Ultrafast Ligand-to-Ligand Electron and Energy Transfer in the Complexes *fac*- $[\text{Re}^{\text{I}}(\text{L})(\text{CO})_3(\text{bpy})]^{n+}$ . *Coord. Chem. Rev.* **2006**, *250*, 1755–1762.

(20) Blanco-Rodriguez, A. M.; Gabrielson, A.; Motevalli, M.; Matousek, P.; Towrie, M.; Sebera, J.; Zalis, S.; Vlcek, A., Jr. Ligand-to-Diimine/Metal-to-Diimine Charge-Transfer Excited States of  $[\text{Re}(\text{NCS})(\text{CO})_3(\alpha\text{-diimine})]$  ( $\alpha\text{-diimine}$  = 2,2'-bipyridine, di- $^i\text{Pr}$ -N,N-1,4-diazabutadiene). A Spectroscopic and Computational Study. *J. Phys. Chem. A* **2005**, *109*, 5016–5025.

(21) Lewis, J. D.; Bussotti, L.; Foggi, P.; Perutz, R. N.; Moore, J. N. Picosecond Forward Electron Transfer and Nanosecond Back Electron Transfer in an Azacrown-Substituted  $[(\text{bpy})\text{Re}(\text{CO})_3(\text{L})]^+$  Complex: Direct Observation by Time-Resolved UV–Visible Absorption Spectroscopy. *J. Phys. Chem. A* **2002**, *106*, 12202–12208.

(22) Partigianoni, C. M.; Chodorowski-Kimmes, S.; Treadway, J. A.; Striplin, D.; Trammell, S. A.; Meyer, T. J. A New Electron-Transfer Donor for Photoinduced Electron Transfer in Polypyridyl Molecular Assemblies. *Inorg. Chem.* **1999**, *38*, 1193–1198.

(23) Perkins, T. A.; Humer, W.; Netzel, T. L.; Schanze, K. S. Solvent-Induced Excited-State Quenching in a Chromophore Quencher Complex. *J. Phys. Chem.* **1990**, *94*, 2229–2232.

(24) Frisch, M. J.; Trucks, G. W.; Schlegel, H. B.; Scuseria, G. E.; Robb, M. A.; Cheeseman, J. R.; Montgomery, J. A., Jr.; Vreven, T.;

Kudin, K. N.; Burant, J. C.; et al. *Gaussian 03*, revision D.02; Gaussian, Inc.: Wallingford, CT, 2004.

(25) Scalmani, G.; Frisch, M. J. Continuous Surface Charge Polarizable Continuum Models of Solvation. I. General Formalism. *J. Chem. Phys.* **2010**, *132*, 114110.

(26) Juris, A.; Balzani, V.; Barigelletti, F.; Campagna, S.; Belser, P.; von Zelewsky, A.  $\text{Ru}(\text{II})$  Polypyridine Complexes: Photophysics, Photochemistry, Electrochemistry, and Chemiluminescence. *Coord. Chem. Rev.* **1988**, *84*, 85–277.

(27) Striplin, D. R.; Crosby, G. A. Photophysical Investigations of Rhenium(I) $\text{Cl}(\text{CO})_3(\text{phenanthroline})$  Complexes. *Coord. Chem. Rev.* **2001**, *211*, 163–175.

(28) Fraser, M. G.; Clark, C. A.; Horvath, R.; Lind, S. J.; Blackman, A. G.; Sun, X.-Z.; George, M. W.; Gordon, K. C. Complete Family of Mono-, Bi-, and Trinuclear  $\text{Re}^{\text{I}}(\text{CO})_3\text{Cl}$  Complexes of the Bridging Polypyridyl Ligand 2,3,8,9,14,15-Hexamethyl-5,6,11,12,17,18-hexaazatrinaphthalene: Syn/Anti Isomer Separation, Characterization, and Photophysics. *Inorg. Chem.* **2011**, *50*, 6093–6106.

(29) Worl, L. A.; Duesing, R.; Chen, P.; Della Ciana, L.; Meyer, T. J. Photophysical Properties of Polypyridyl Carbonyl Complexes of Rhenium(I). *J. Chem. Soc., Dalton Trans.* **1991**, 849–858.

(30) Nakamoto, K. *Infrared and Raman Spectra of Inorganic and Coordination Compounds*; Wiley: New York, 1997; pp 272–280.

(31) Horng, M. L.; Gardecki, J. A.; Papazyan, A.; Maroncelli, M. Subpicosecond Measurements of Polar Solvation Dynamics - Coumarin-153 Revisited. *J. Phys. Chem.* **1995**, *99*, 17311–17337.

(32) Hamm, P.; Ohline, S. M.; Zinth, W. Vibrational Cooling after Ultrafast Photoisomerization of Azobenzene Measured by Femtosecond Infrared Spectroscopy. *J. Chem. Phys.* **1997**, *106*, 519–529.

(33) Hamm, P.; Ohline, S.; Zurek, M.; Roschinger, T. Vibrational Cooling after Photoisomerization: First Application of a Novel Intramolecular Thermometer. *Laser Chem.* **1999**, *19*, 45–49.

(34) Ma, C.; Kwok, W. M.; Matousek, P.; Parker, A. W.; Phillips, D.; Toner, W. T.; Towrie, M. Time-Resolved Study of the Triplet State of 4-Dimethylaminobenzonitrile (DMABN). *J. Phys. Chem. A* **2001**, *105*, 4648–4652.

(35) Huang, J.; Stockwell, D.; Huang, Z.; Mohler, D. L.; Lian, T. Photoinduced Ultrafast Electron Transfer from CdSe Quantum Dots to Re-bipyridyl Complexes. *J. Am. Chem. Soc.* **2008**, *130*, 5632–5633.

(36) Grills, D. C.; Cook, A. R.; Fujita, E.; George, M. W.; Preses, J. M.; Wishart, J. F. Application of External-Cavity Quantum Cascade Infrared Lasers to Nanosecond Time-Resolved Infrared Spectroscopy of Condensed-Phase Samples Following Pulse Radiolysis. *Appl. Spectrosc.* **2010**, *64*, 563–570.

(37) Smieja, J. M.; Kubiak, C. P.  $\text{Re}(\text{bipy-tBu})(\text{CO})_3\text{Cl}$ -Improved Catalytic Activity for Reduction of Carbon Dioxide: IR-Spectroelectrochemical and Mechanistic Studies. *Inorg. Chem.* **2010**, *49*, 9283–9289.

(38) Roy, S.; Kubiak, C. P. Tricarbonylrhenium(I) Complexes of Highly Symmetric Hexaazatrinaphthylene Ligands (HATN): Structural, Electrochemical and Spectroscopic Properties. *Dalton Trans.* **2010**, *39*, 10937–10943.

(39) Gabrielson, A.; Matousek, P.; Towrie, M.; Hartl, F.; Zalis, S.; Vlcek, A., Jr. Excited States of Nitro-Polypyridine Metal Complexes and Their Ultrafast Decay. Time-Resolved IR Absorption, Spectroelectrochemistry, and TD-DFT Calculations of *fac*- $[\text{Re}(\text{Cl})(\text{CO})_3(5\text{-nitro-1,10-phenanthroline})]$ . *J. Phys. Chem. A* **2005**, *109*, 6147–6153.

(40) Rossenaar, B. D.; Hartl, F.; Stufkens, D. J. Reduction of  $[\text{Re}(\text{X})(\text{CO})_3(\text{R}'\text{-DAB})]$  (X =  $\text{Otf}^-$ ,  $\text{Br}^-$ ; DAB = Diazabutadiene;  $\text{R}'$  =  $^i\text{Pr}$ , pTol, pAn) and  $[\text{Re}(\text{R})(\text{CO})_3(\text{iPr-DAB})]$  (R = Me, Et, Bz) Complexes: A Comparative (Spectro)electrochemical Study at Variable Temperatures. *Inorg. Chem.* **1996**, *35*, 6194–6203.